

Visco- and plasto-elastic fracture of nano-porous polymer sheets

Takako Tomizawa and Ko Okumura

Department of Physics, Ochanomizu University, Tokyo, Japan

(Dated: March 27, 2019)

Abstract

We study the dependence of the fracture surface energy on the pulling velocity for nano-porous polypropylene (PP) sheets to find two components: the static and dynamic ones. We show that these terms can be interpreted respectively as plastoelastic and viscoelastic components, as has been shown for soft polyethylene (PE) foams in a previous work. Considering significant differences in the pore size, volume fraction and Young's modulus of the present PP and previous PE sheets, the present results suggest a universal physical mechanism for fracture of porous polymer sheets. The simple physical interpretation emerging from the mechanism could be useful for developing tough polymers. Equivalence of Griffith's energy balance in fracture mechanics to a stress criterion is also discussed and demonstrated using the present experimental data.

I. INTRODUCTION

Cellular solids, which are porous materials with a well-defined pore size, are found in natural and artificial materials and are a useful form of materials [1]. Cork, balsa, and apples [2] are cellular solids originated from plants, and the stereom of echinoderms [3], skeleton of a certain sponge [4], and frustule of diatoms [5] are examples from creatures. Such materials possess mechanical advantages because they can be light, strong, shock-absorbing, and heat-retaining. Accordingly, active studies have been performed on mechanical and fracture mechanical properties, focusing on an important parameter for cellular solids, the volume fraction of the matrix material ϕ [1]. However, studies on velocity dependent properties of their fracture are relatively limited, compared with intensive studies that have been performed on other materials such as adhesive [6–10], laminar [11], viscoelastic [12, 13], weakly cross-linked [14, 15], biopolymer gel [16], and biological composite [17] materials, including recent active experimental [18–20], numerical [21, 22], and theoretical [23, 24] studies on the velocity jump in crack propagation in elastomers.

Previously, we studied mechanical and fracture mechanical properties of soft solidified foam of non-cross-linked polyethylene. Young’s modulus E , the characteristic pore size d_0 , and the volume fraction ϕ of the foams were of the orders of 1 MPa, 1 mm, and 0.03, respectively. For the soft foams, we established scaling laws for Young’s modulus and the fracture surface energy as a function of ϕ . The scaling laws thus found are different from the ones established for well-studied hard cellular solids of Young’s modulus typically around 3000 MPa [25]. Furthermore, we revealed for the same soft solidified foams a simple relation between the fracture surface energy (required at the crack initiation) and pulling velocity with a clear physical interpretation [26]. Here, we test this simple description for the velocity dependence of the fracture energy, using a porous polymer of different nature. The present sample is not polyethylene (PE) but polypropylene (PP) and E , d , and ϕ in the present case are significantly different from those in the previous study: $E \sim 200$ MPa, $d_0 \sim 1 \mu\text{m}$, and $\phi \sim 0.5$. As a result, we find that the same description is well-applicable for this quite different material and suggest that the simple description proposed in the previous study can be universally relevant to a certain class of porous polymers.

II. EXPERIMENTAL SECTION

A. Materials.

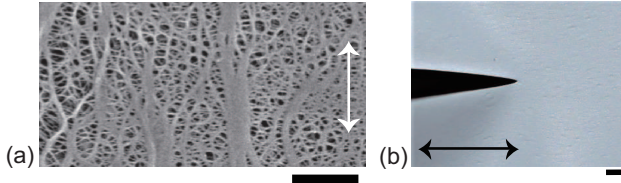


FIG. 1. (a) A SEM image of the porous polypropylene sheet used in the experiment (Copyright 2018 by Mitsubishi Chemical Corporation). The length of the scale bar is $1\ \mu\text{m}$. (b) Magnified view near a crack tip. The machine direction are shown by double-headed arrows, which is perpendicular to the pulling direction. The length of the scale bar is $1\ \text{mm}$.

In this experiment, we use sheets of polypropylene (PP) that possesses a porous structure as shown in Fig. 1(a). The structure may be characterized by a few different length scales and the largest scale is around $1\ \mu\text{m}$, which could be comparable to $10^{-5}\ \text{m}$, as seen from the SEM image. The volume fraction ϕ and the thickness of the sheet are 0.44 and $23\ \mu\text{m}$, respectively. The sheet is fabricated from bulk with a stretching process and thus tends to be stronger in the direction, which will be called the machine direction.

B. Mechanical measurement

The elongation of a sheet from the natural length and the tensile force acting on the sheet were measured with a hand-made setup, which was used in our previous study [26]. This setup is equipped with horizontally placed two pairs of clamp bars specially designed for sheet samples of dimension comparable to $50\ \text{cm}$ to avoid any slips at the clamps and local slacking of a sheet sample under stretch. The horizontal width of the sample is $10\ \text{cm}$ for failure stress measurements ($5\ \text{cm}$ for force-extension measurements) and the vertical height, i.e., the distance between the inner edges of the clamp bars is $12.5\ \text{cm}$. The bottom pairs of clamp bars are fixed to the setup frame, while the position and speed of the mobile upper pairs of clamp bars can be controlled by a slider system (EZSM6D040 K, Oriental Motor) through a digital force gauge (FCC-50B, NIDEC-Shimpo). Each measurement is performed

for a given fixed velocity of the upper clamp, which defines the pulling velocity V . All the experiments are performed with setting the machine direction perpendicular to the vertical direction, in which direction the constant stretching speed V is given by the controlled slider system. The pulling velocity V is varied from 0.03 mm/sec to 0.4 mm/sec.

Fracture mechanical measurements are performed with the same setup but with introducing a macroscopic line crack with a sharp knife at the center of the sample (see Fig. 1(b)). The line crack is created in the horizontal direction (i.e., the machine direction) and the length $2a$ is varied from 2 to 32 mm.

III. RESULTS

A. Stress-strain curve and Young's modulus

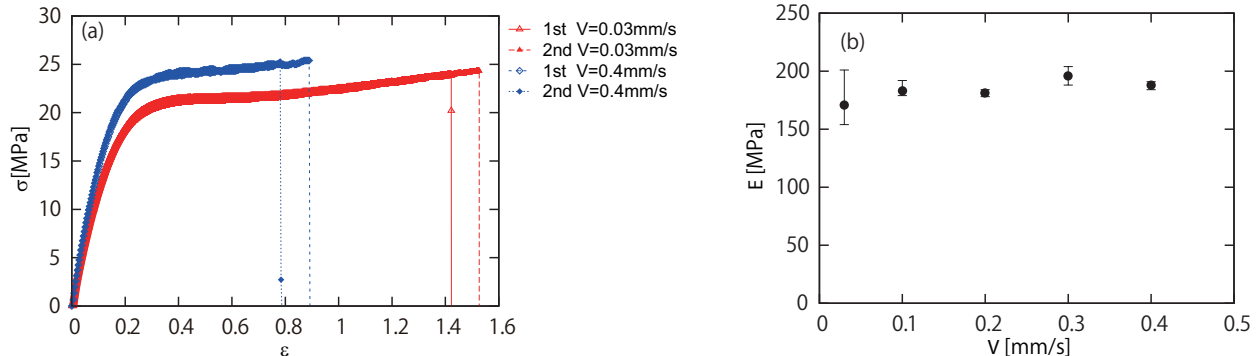


FIG. 2. (a) Stress-strain curves obtained from the force-extension measurements performed with samples without any macroscopic cracks at extension velocities, $V = 0.03$ and 0.4 mm/sec. (b) Young's modulus E determined in the initial regime in the stress-strain curve as a function of the stretching velocity V .

Figure 2(a) shows typical results for the relation between stress σ and strain ϵ of the sheet sample at different velocities. Nearly overlapped two data sets at each velocity show a reasonable reproducibility of the experiment. The relation shows a weak nonlinearity with a weak dependence of velocity. However, in the initial regime in which ϵ and σ are less than ~ 0.1 and ~ 2 MPa, respectively, the relation is almost linear and is almost independent of velocity. In fact, Young's modulus extracted from this region is practically constant as

shown in Fig. 2(b). Here, the modulus at each velocity is determined as the average of the three moduli obtained from the initial regimes of three sets of force-elongation measurements performed at each velocity, with the bottom and top values of each error bar showing the minimum and maximum of the three results.

B. Failure stress with a line crack and fracture surface energy

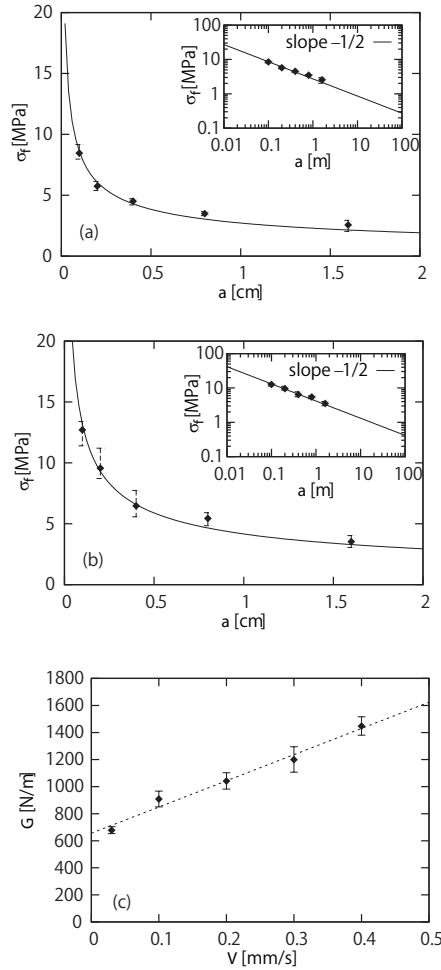


FIG. 3. Failure stress σ_f as a function of crack size $2a$ at $V = 0.03$ mm/sec (a) and $V = 0.4$ mm/sec (b). The insets show corresponding plots on a log-log scale. (c) Fracture surface energy G as a function of velocity V .

Figure 3(a) and (b) show typical results for the relation between the failure stress σ_f and the half length of the line crack a . The measurement of σ_f for given a and V are performed

three times and the average of the three values is plotted with an error bar in the figure. When data are plotted on a log-log scale, the data for a given V collapse clearly on a straight line with slope $-1/2$. This justifies that we use the following Griffith's formula to estimate the fracture surface energy G for a given V [27]:

$$\sigma_f = \left(\frac{2EG}{\pi a} \right)^{1/2} \quad (1)$$

Figure 3(c) shows the relation between the pulling velocity V and the fracture surface energy G on the basis of Eq. (1). The relation can be well described by the linear form: $G = A + BV$. Here, A and B are constants independent of V . On the other hand, it is theoretically justified and experimentally confirmed that G is proportional to the volume fraction ϕ [25, 26]. Exploiting this property, we rewrite the expression $G = A + BV$ in the following form:

$$G = \phi G_0 (1 + V/V_0) \quad (2)$$

with introducing G_0 and V_0 , which are independent of V (G_0 and V_0 are defined by the relations $A = \phi G_0$ and $B = \phi G_0/V_0$).

In the following, we justify that the above expression can be reasonably well interpreted as in the following form:

$$G = \phi(\sigma_Y + \eta(V/d))\delta \quad (3)$$

We examine the validity of the above expression at the level of scaling laws. For simplicity we regard $\phi \sim 1$ and ignore this factor in the following. The first term $\phi\sigma_Y\delta \sim \sigma_Y\delta$ is considered as the standard expression for plastic fracture with σ_Y the yield stress and δ is the crack opening distance [27]. Considering a typical value of σ_Y for PP, say, 50 MPa, the opening distance δ can be estimated as $\sim 10^{-5}$ m because $\phi G_0 \sim G_0$ ($\sim \sigma_Y\delta$) is estimated as 650 J/m² from Figure 3(c). This value of δ is comparable to the largest characteristic scale of the porous structure in the sample; it is quite natural that we expect that crack opening distance scale as this length scale. The second term, in particular the quantity $\eta(V/d)$, just describe the viscous stress that we have to add to σ_Y in the dynamic case. Here, d describes the length scale around the crack tip dynamically affected and it is natural to assume that this scale as δ . Taking the viscous effect into account is reasonable because the glass transition temperature of PP is well below ambient temperature (typically 0 °C),

at which the experiments were performed and the viscosity η is estimated as 2×10^6 Pa.s from Figure 3(c) by estimating the value $\phi G_0/V_0 \sim G_0/V_0$, which scale as $\eta\delta/d \sim \eta$. To gain physical insight, we can roughly estimate the number of monomers N in the entangled polymer by invoking the reptation model [28]. This crude estimate gives $\eta \sim \eta_0 N^3/N_e^2$ with N_e the entangle distance (~ 100) and η_0 the viscosity of monomers (~ 1 mPa.s). As a result, we obtain a plausible value, $N \sim 10^4$. Since we have established the same reasoning for Eq. (3) in Ref.[26] for soft foam sheets of polyethylene, the present result suggests a certain degree of universality of Eq. (3). Our result suggests that the dynamic toughness is significantly increased if the number of monomers N is increased, because the velocity dependent term in G contains the viscosity η and, even if the reptation model is not appropriate, η is strongly dependent on N .

Equation (3) established as above can be interpreted as composed of the static term reflecting a plastoelastic effect and the dynamic term reflecting a viscoelastic effect, as explained as follows. This expression is composed of two terms, one independent of V and the other dependent on V . In other words, G is composed of the static and dynamic parts. The static part reflects a plastic effect because it is proportional to the yield stress σ_Y . The dynamic part corresponds to viscous effect because it originates from viscous stress. On the other hand, G in the present study is determined by linear-elastic fracture mechanics. Therefore, it is natural to interpret the static and dynamic terms as plastoelastic and viscoelastic effects, respectively.

IV. EQUIVALENCE OF GRIFFITH ENERGY BALANCE TO A STRESS CRITERION

As we discussed in our previous paper, the energy balance is equivalent to a stress criterion, if we note that the stress concentration is cutoff at the length scale below which the continuum description fails, although Griffith's energy balance is sometimes distinguished from the stress criteria for fracture. (This length scale corresponds to the largest scale characterizing the porous structure and, thus, will be called d in the following.) This can be experimentally confirmed for the present material. To see this, let us briefly review how the energy balance reduces to a stress criterion. We introduce a critical failure stress σ_c for a

given material through the following relation:

$$\sigma_c \simeq (EG/d)^{1/2} \quad (4)$$

This comes from the well-known Griffith's formula for the failure stress $\sigma_f \simeq (EG/a)^{1/2}$ for a crack of length $\sim a$ and the idea of Griffith's cavities. We further introduce the maximum stress that appears at the crack tip at the critical of failure at which the remote stress σ_0 is equal to the failure stress σ_f :

$$\sigma_m \simeq \sigma_f(a/d)^{1/2} \quad (5)$$

This comes from the well-known Inglis' stress concentration formula for the stress distribution around a crack $\sigma(r) \simeq \sigma_0(a/r)^{1/2}$ at a distance r from the crack tip, which should be cutoff at the scale d . (This relation $\sigma(r) \simeq \sigma_0(a/r)^{1/2}$ has been confirmed in previous numerical studies [29, 30].) The stress criteria that is equivalent to Griffith's energy balance is then given by

$$\sigma_c \simeq \sigma_m \quad (6)$$

In fact, from Eqs. (4) to (6), we recover Griffith's formula.

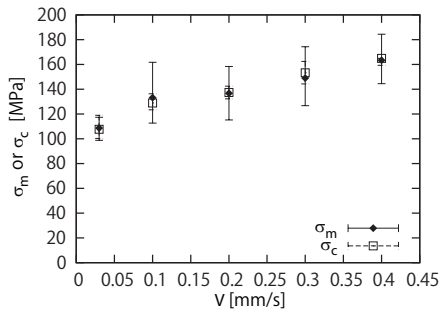


FIG. 4. σ_c vs σ_m .

To confirm the above description is relevant to the present experiment, we experimentally determine σ_c and σ_m , respectively, from Eq. (4) (using measured values of E , G , and d) and from Eq. (5) (using measured values of σ_f , a , and d). We here set the coefficient for Eq. (4) to be 1 and that for Eq. (5) to be 0.841 and use $d = 10^{-5}$ m for both equations, for simplicity. (If we denote dimensionless numerical coefficients suppressed in Eq. (4) to Eq. (6) as c_4 , c_5 , and c_6 , respectively, Eq. (6) can be expressed as $(EG/d)^{1/2} = (c_6c_5/c_4)\sigma_f(a/d)^{1/2}$, which implies c_6c_5/c_4 is close to 0.841.) The results are shown in Fig. 4, which confirms that the stress criteria Eq. (6) is satisfied for the experimentally observed fractures and, thus, the above description is consistent with our experimental results.

V. CONCLUSION

We have studied the fracture surface energy at the onset of crack initiation as a function of the pulling velocity. As a result, we find that the fracture energy is described by the static and dynamic components. The former corresponds to the standard plastic fracture. The latter reflects the viscous flow that occurs at the crack tip. The both components are characterized by the length scale that is comparable to the pore size. The existence of the dynamic and viscous component suggests a simple principle for toughening: the increase in the degree of polymerization could greatly enhance the dynamic toughness. The equivalence of Griffith's energy balance to a stress criterion is also demonstrated. These results are completely in parallel with the results obtained for significantly different porous polymer sheets, which suggests the universality of the present results although further studies will be needed to clarify the limitation of the present interpretation.

Considering that the basic physical properties of polymer materials are quite dependent on preparation crystallinity, molecular orientation, size and shape of porous structure, types of polymers [31], the emergence of this kind of universality may be unexpected. (The fracture of crystalline polymers on microscopic scales are started to be reproduced in simulations [32].) We consider that one of the reasons for this universality comes from that we introduce a macroscopic crack, whose scale is much larger the characteristic scales for such as crystallinity, domains in which molecules are oriented and porous structure. On such a macroscopic scale, it is known that polymers universally exhibit yielding and viscous flowing in a similar manner. When these points are considered, it would not be so surprising if the fracture associated with a macroscopic crack has universally governed by yielding and viscous flowing in their simplest forms, which we are suggesting.

The study concerns the fracture surface energy required at the onset of crack initiation. Such a fracture energy should be in general distinguished from the fracture energy required during crack propagation. In fact, recently, we have studied the relation between the energy release rate, which can be interpreted as the fracture surface energy required during crack propagation, and the crack-propagation velocity, for the same material studied in the present study [33]. As a result, we did not observe crack propagation in the velocity range studied in the present study. However, in the previous study [33], from a technical reason, the constant-speed crack propagation with a fixed-grip condition was initiated some time after

we set a given strain to samples and we consider that the effect of stress relaxation due to this preparation time could tend to suppress crack propagation. This point will be further discussed elsewhere.

ACKNOWLEDGEMENTS

The authors are grateful to Mitsubishi Chemical Corporation for providing nano-porous sheet samples and the SEM image shown in Fig. 1(a). The authors thank Dr. Atsushi Takei for technically helping them for experiments. This work was partly supported by ImPACT Program of Council for Science, Technology and Innovation (Cabinet Office, Government of Japan).

-
- [1] Lorna J Gibson and Michael F Ashby. *Cellular solids: structure and properties*. Cambridge Univ. Press., Cambridge, U.K., 1999.
 - [2] A.L.I.A. Khan and J.F.V. Vincent. Mechanical damage induced by controlled freezing in apple and potato. *J. Texture Studies*, 27(2):143–157, 1996.
 - [3] R.B. Emlet. Echinoderm calcite: a mechanical analysis from larval spicules. *Biol. Bull.*, 163(2):264–275, 1982.
 - [4] J. Aizenberg, J.C. Weaver, M.S. Thanawala, V.C. Sundar, D.E. Morse, and P. Fratzl. Skeleton of euplectella sp.: structural hierarchy from the nanoscale to the macroscale. *Science*, 309(5732):275–278, 2005.
 - [5] Christian E Hamm, Rudolf Merkel, Olaf Springer, Piotr Jurkojc, Christian Maier, Kathrin Prechtel, and Victor Smetacek. Architecture and material properties of diatom shells provide effective mechanical protection. *Nature*, 421(6925):841–843, 2003.
 - [6] AN Gent and J Schultz. Effect of wetting liquids on the strength of adhesion of viscoelastic material. *The Journal of Adhesion*, 3(4):281–294, 1972.
 - [7] Manoj K Chaudhury. Rate-dependent fracture at adhesive interface. *The Journal of Physical Chemistry B*, 103(31):6562–6566, 1999.
 - [8] Yoshihiro Morishita, Hiroshi Morita, Daisaku Kaneko, and Masao Doi. Contact dynamics in the adhesion process between spherical polydimethylsiloxane rubber and glass substrate.

- Langmuir*, 24(24):14059–14065, 2008.
- [9] Costantino Creton, Edward Kramer, Hugh Brown, and Chung-Yuen Hui. Adhesion and fracture of interfaces between immiscible polymers: from the molecular to the continuum scale. *Adv. Polymer Sci.*, 156:53–136, 2002.
- [10] Satyam Bhuyan, François Tanguy, David Martina, Anke Lindner, Matteo Ciccotti, and Costantino Creton. Crack propagation at the interface between soft adhesives and model surfaces studied with a sticky wedge test. *Soft Matter*, 9(28):6515–6524, 2013.
- [11] AJ Kinloch, CC Lau, and JG Williams. The peeling of flexible laminates. *International Journal of Fracture*, 66(1):45–70, 1994.
- [12] JA Greenwood and KL Johnson. The mechanics of adhesion of viscoelastic solids. *Phil. Mag. A*, 43(3):697–711, 1981.
- [13] RA Schapery. A theory of crack initiation and growth in viscoelastic media. *International Journal of Fracture*, 11(1):141–159, 1975.
- [14] PG de Gennes. *C. R. Acad. Sci. Paris*, 307:1949, 1988.
- [15] F Saulnier, T Ondarcuhu, A Aradian, and Et Raphaël. Adhesion between a viscoelastic material and a solid surface. *Macromolecules*, 37(3):1067–1075, 2004.
- [16] Maxime Lefranc and Elisabeth Bouchaud. Mode I fracture of a biopolymer gel: Rate-dependent dissipation and large deformations disentangled. *Extreme Mechanics Letters*, 1:97–103, 2014.
- [17] Eran Bouchbinder and Efim A Brener. Viscoelastic fracture of biological composites. *Journal of the Mechanics and Physics of Solids*, 59(11):2279–2293, 2011.
- [18] K Tsunoda, JJC Busfield, CKL Davies, and AG Thomas. Effect of materials variables on the tear behaviour of a non-crystallising elastomer. *J. Mater. Sci.*, 35(20):5187–5198, 2000.
- [19] Yoshihiro Morishita, Katsuhiko Tsunoda, and Kenji Urayama. Velocity transition in the crack growth dynamics of filled elastomers: Contributions of nonlinear viscoelasticity. *Physical Review E*, 93(4):043001, 2016.
- [20] Yoshihiro Morishita, Katsuhiko Tsunoda, and Kenji Urayama. Crack-tip shape in the crack-growth rate transition of filled elastomers. *Polymer*, 108:230–241, 2017.
- [21] Atsushi Kubo and Yoshitaka Umeno. Velocity mode transition of dynamic crack propagation in hyperviscoelastic materials: A continuum model study. *Scientific Reports*, 7:42305, 2017.

- [22] Yuko Aoyanagi and Ko Okumura. Stationary crack propagation in a two-dimensional viscoelastic network model. *Polymer*, 120:94–99, 2017.
- [23] Naoyuki Sakumichi and Ko Okumura. Exactly solvable model for a velocity jump observed in crack propagation in viscoelastic solids. *Scientific Reports*, 7(1):8065, 2017.
- [24] Ko Okumura. Velocity jumps in crack propagation in elastomers: Relevance of a recent model to experiments. *Journal of the Physical Society of Japan*, 87(12):125003, 2018.
- [25] Y. Shiina, Y. Hamamoto, and K. Okumura. Fracture of soft cellular solids - case of non-crosslinked polyethylene foam. *Europhys. Lett.*, 76(4):588–594, 2006.
- [26] Yuki Kashima and Ko Okumura. Fracture of soft foam solids: Interplay of visco-and plasto-elasticity. *ACS Macro Lett.*, 3:419–422, 2014.
- [27] T.L. Anderson. *Fracture Mechanics 3rd ed.* CRC Press, Boca Raton, Florida, 2005.
- [28] Pierre Gilles De Gennes. *Scaling concepts in polymer physics.* Cornell Univ. Press, Ithaca, NY, 1979.
- [29] S. Nakagawa and K. Okumura. Crack-tip stress concentration and mesh size in networks. *J. Phys. Soc. Jpn.*, 76(11):4801, 2007.
- [30] Y. Aoyanagi and K. Okumura. Crack-tip stress concentration and structure size in nonlinear structured materials. *J. Phys. Soc. Jpn.*, 78(3):034402, 2009.
- [31] Gert R Strobl and Gert R Strobl. *The physics of polymers*, volume 2. Springer, 1997.
- [32] Yuji Higuchi. Fracture processes of crystalline polymers using coarse-grained molecular dynamics simulations. *Polymer Journal*, page 1, 2018.
- [33] Atsushi Takei and Ko Okumura. Crack propagation in porous polymer sheets with different pore sizes. *MRS Communications*, pages 1–6, 2018; <http://dx.doi.org/10.1557/mrc.2018.222>.